CHEMISTRY
A European Journal

Accepted Article

Title: 2,2'-Bipyridine Equipped with a Disulfide/Dithiol Switch for Coupled Two Electron and Proton Transfer

Authors: Mauricio Cattaneo, Christine Schiewer, Anne Schober, Sebastian Dechert, Inke Siewert, and Franc Meyer

This manuscript has been accepted after peer review and appears as an Accepted Article online prior to editing, proofing, and formal publication of the final Version of Record (VoR). This work is currently citable by using the Digital Object Identifier (DOI) given below. The VoR will be published online in Early View as soon as possible and may be different to this Accepted Article as a result of editing. Readers should obtain the VoR from the journal website shown below when it is published to ensure accuracy of information. The authors are responsible for the content of this Accepted Article.

WILEY-VCH

FULL PAPER

2,2'-Bipyridine Equipped with a Disulfide/Dithiol Switch for Coupled Two Electron and Proton Transfer

Mauricio Cattaneo,[a,b]§* Christine E. Schiewer,[a]§ Anne Schober,[a] Sebastian Dechert,[a] Inke Siewert,[a,c]* and Franc Meyer[a,c]*

Dedicated to Prof. Dr. Wolfgang Schnick on the occasion of his 60th birthday

Abstract: [1,2]dithiino[4,3-b:5,6-b']dipyridine (**1**) and its protonated open form 3,3'-dithiol-2,2'-bipyridine (**2**) were synthesised and their interconversion investigated. The X-ray structure of **2** revealed an *anti* orientation of the two pyridine units and a zwitterionic form. In depth electrochemical studies in combination with DFT calculations lead to a comprehensive picture of the redox chemistry of **1** in the absence and presence of protons. Initial one electron reduction at E_1 = −1.97 V results in the formation of the radical anion **1^{red}** with much elongated S–S bond, which readily undergoes further reduction at E_2 = −2.15 V. Water triggers a potential inversion ($E \geq -1.9$ V for the second reduction) as the radical anion **1^{red}** is protonated at its basic N atom. DFT studies revealed that S–S bond breaking and twisting of the pyridine units generally occurs after the second reduction step while the potential inversion induced by protonation is a result of charge compensation. The CV data were simulated to derive rate constants for the individual chemical and electrochemical reactions for both scenarios in the absence and presence of protons.

Introduction

Dithiol/disulfide interconversions play an important role for redox control and charge storage in biochemical systems.[1] Inspired by nature, organic molecules have been designed that make use of the dithiol/disulfide switch for multiple electron storage in material science. In that context, dithiins appear to be particularly promising, and their electrochemistry has been studied in detail;[2] recently reported systems A − C relevant to the present work are shown in Fig. 1.[3,4,5] Questions of general interest address the sequence of events during disulfide reduction and how S–S bond breakage is correlated with electron injection and protonation, as well as the combination with potential internal electron transfer processes involving other reducible

moieties such as the viologen part in **C**.[4,5] Three different mechanisms have been discussed for reductive S−S cleavage processes in diaromatic disulfide compounds, namely an ECE,[6] EE,[5] or an EEC[3] mechanism. An ECE mechanism has been observed in diaryl disulfides such as (C$_6$H$_5$S)$_2$ and its *para* substituted derivatives.[6] EE and EEC mechanisms have been proposed for dithiins **A** and **B**, respectively. The initial reduction of **A** and **B** leads to S−S bond elongation, while the respective second reductions have substantially higher reduction potentials than the first ones and initiate rapid S−S bond cleavages.[3,5] In case of **A**, quantum chemical studies suggested a mechanism switch from EEC to ECE in the presence of protons.[3b]
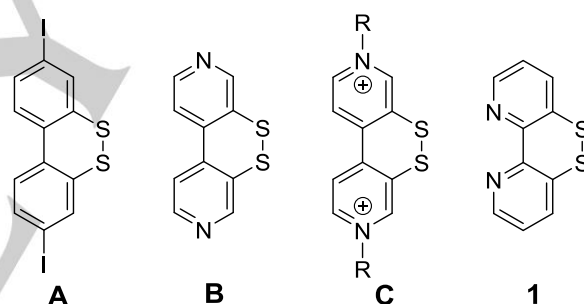

Fig. 1 Previously studied dithiines **A** − **C**[3,4,5] and the new 2,2'-bipyridine derivative **1**.

We here report the synthesis of new dithiine **1** that is related to **B** but amalgamates the disulfide/dithiol switch with the versatile 2,2'-bipyridine metal binding capabilities.[7] 2,2'-Bipyridines are among the most widely used ligands in coordination chemistry, with manifold substitutions and modifications being reported for tuning their electronic and steric properties, or for other functionalization.[8] As charge transfer processes and key steps in redox catalysis are often associated with proton transfers, efforts have been made to add to metal complexes with bipyridine-type ligands the potential for proton coupled electron transfer (PCET) reactivity by substituting one of the pyridine rings by, e.g., imidazole or imidazoline.[9] Such elaboration of bipy-type ligands is expected to be beneficially exploited in solar fuel generation or other solar-energy conversions. The new 2,2'-bipyridine derivative **1** that is equipped with a disulfide/dithiol switch in the 3,3'-positions of the chelate ligand will be particular useful in this context as it potentially mediates two electron conversion via reversible S–S bond breaking and making, triggered or coupled to proton transfer. In depth understanding of the fundamental 2e$^−$/2H$^+$

[a]   Prof. F. Meyer, Prof. I. Siewert, Dr. M. Cattaneo, Dr. S. Dechert, C.
       E. Schiewer, A. Schober, Institut für Anorganische Chemie,
       Universität Göttingen, Tammannstr. 4, D-37077 Göttingen.
       E-mail: franc.meyer@chemie.uni-goettingen.de,
       inke.siewert@chemie.uni-goettingen.de
[b]   Dr. M. Cattaneo, Instituto de Quimica Fisica, Universidad Nacional
       de Tucumán, Ayacucho 471, T4000INI San Miguel de Tucumán,
       Argentina. E-mail: mcattaneo@fbqf.unt.edu.ar
[c]   Prof. F. Meyer, Prof. I. Siewert, International Center for Advanced
       Studies of Energy Conversion (ICASEC), Universität Göttingen,
       D-37077 Göttingen
§   these authors contributed equally to the work

       Supporting information for this article is given via a link at the end of
       the document.

chemistry of the new bipyridine derivate is a prerequisite for its application towards PCET processes in coordination chemistry.

In this contribution, we rigorously examine the redox properties and interconversion of **1** and its 2e⁻/H⁺ reduced dithiol congener **2**. In particular, the effect of protons on the redox chemistry is addressed to reveal a detailed picture of the individual chemical and electrochemical steps.

Results and Discussion

1 was synthesised via a three step protocol (Scheme 1) starting from 3,3'-dihydroxy-2,2'-bipyridine, using Newman-Kwart rearrangement (**I→II**) in close analogy to the procedures developed previously for the 4,4'-bipyridine analogoue **B**[4] and 3,8-diiodo-dibenzo[1,2]dithiine **A**.[3] Careful optimization of the reaction conditions (time, temperature) was required to minimize the amount of side products (mainly the singly rearranged precursor compound (**IV**) and the monosulfur decay product **III**), from which the desired twice rearranged **II** needs to be separated. **I**, **II**, and **III** have been fully characterized and structurally authenticated (see Supporting Information). Reductive removal of the dimethylcarbamoyl groups in **II** has to be performed under anaerobic conditions for isolating 2,2'-bipyridine-3,3'-dithiol **2**; in presence of O₂ the target dithiine **1** is readily formed.
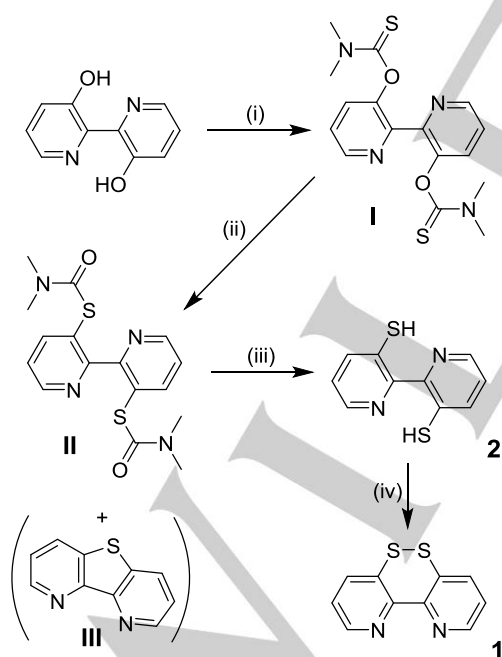
Scheme 1 Synthesis of **2** and **1**. (i) 1. NaH, DMF; 2. Me₂NC(S)Cl, DMF, 85°C. (ii) 280°C, 7 min. (iii) 1. LiAlH₄, THF; 2. HCl. (iv) O₂, CH₂Cl₂.

Few single crystals of **2** could be obtained, and its molecular structure was determined (Fig. 2). X-ray diffraction shows

that the zwitterionic form is preferred, similar to what has been reported for 3-mercaptopyridine.[10,11] Dithiine **1** is stable in neutral and acidic degassed water, however, under strongly basic conditions it transforms into thieno[3,2-b:4,5-b']bipyridine **III**. NMR monitoring and MS/MS experiments suggest this decomposition to proceed via nucleophilic attack of hydroxide ions at the disulfide bond of **1**, leading to 3'-mercapto-[2,2'-bipyridine]-3-sulfinic acid as an intermediate[12] which, upon prolonged standing of the solution, finally converts to **III** (SI Fig. S11 and S12).
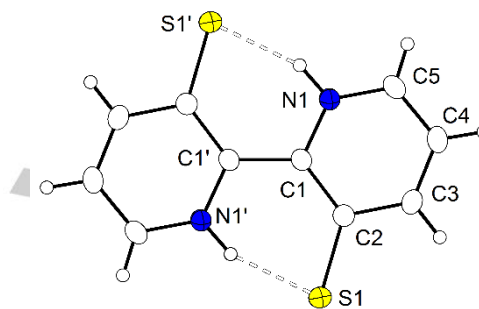
Fig. 2 Molecular structure of **2** in solid state (50% probability ellipsoids). Selected atom distances: S1–C2 1.7318(16); N1–C1 1.357(2); N1···S1' 2.8844(15) Å. Symmetry transformation used to generate equivalent atoms: (') 1-x, 1–y, 1-z. Crystallographic details as well as further bond lengths and angles can be found in the SI.

The solution UV/vis spectrum of pale yellow **1** in buffered, neutral water shows two intense bands at 270 and 305 nm and a weaker, broad absorption at 380 nm; the former are assigned to π-π* transitions which occur at energies similar to those of the π-π* absorptions of 2,2-biphenyldisulphide,[13] while the broad band at lower energy likely originates from n-π* transitions. Protonation of **1** causes a bathochromic shift of all bands to 279, 322, and 423 nm,[14] which intensifies the yellow color. Isosbestic points indicate clean interconversion between **1** and its protonated form **[1H]⁺**, and pH dependent UV/vis titrations revealed one protonation equilibrium with a pK_a of 2.88(1) (Fig. 3). This is in good agreement with spectrofluorometric titration data which show a red-shift of the emission band of **1** from 365 to 420 nm upon lowering the solution pH (a fit of the spectrofluorometric data suggests a pK_a* of 2.60(5); Fig. S6 in the SI). ¹⁵N NMR spectroscopy confirms the bipyridine-N as the protonation site, reflected by a shift from δ = −70 ppm in **1** to −135 ppm in **[1H]⁺**. The ¹H NMR spectrum shows apparent C_{2v} symmetry of the protonated species, which is in line with fast H⁺-tautomerism between the two N atoms. The pK_a value of **1** is lower than that of parent 2,2'-bipyridine (*cf.* pK_a = 4.45)[15] or phenanthroline (*cf.* pK_a = 4.84),[16] but such low pK_a value has precedents in literature for some pyridine derivatives.[17] In MeCN, titration of **1** with strong acids such as trifluoromethanesulfonic acid (TfOH) suggests twofold protonation, while the weak acid benzoic acid does not lead to protonation (Fig. S8-S10).
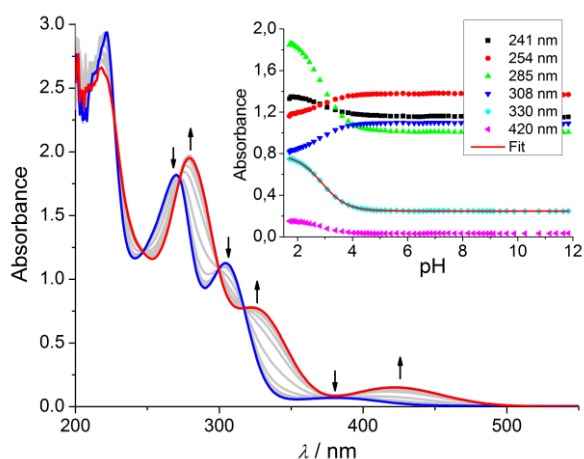
Fig. 3 Spectrophotometric pH-titration of **1** in aqueous Britton-Robinson buffer; red: pH = 1.8, blue: pH = 10.

1 shows two irreversible oxidation features peaking at 1.16 V and 1.60 V, and one reduction feature with a maximum peak potential of −1.66 V and a re-oxidation wave at −0.74 V at a scan rate of 0.1 Vs^{-1} (Fig. 4, all potentials are reported *vs.* Fc$^{+/0}$). The two one-electron oxidations of **1** likely result in the formation of the corresponding dithione, (Z)-3H,3'H-[2,2'-bipyridinylidene]-3,3'-dithione, as it is commonly observed in related systems.[12,18] The absolute value of the peak current $I_{p,c}$ of the reduction wave increased linearly with the square root of the scan rate (0.1 − 10 Vs^{-1}), which is characteristic for a diffusion controlled process (Fig. 4, inset). The large separation of the cathodic and the corresponding anodic wave and the linear shift of the cathodic peak potential $E_{p,c}$ per log(v) is indicative for either irreversible electron transfer processes or (ir)reversible electron transfer processes followed by a fast chemical reaction (Fig. S13).[19]
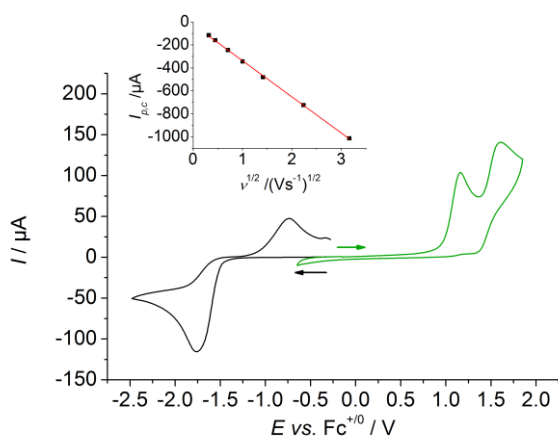

Fig. 4 Cyclic voltammogram of **1** in acetonitrile at rt (I = 0.1 M Bu$_4$NPF$_6$, [**1**] = 3.1 mM), v = 0.1 Vs^{-1}. The inset shows a plot of the peak current $I_{p,c}$ *vs.* the square root of the scan rate for the cathodic process.

A coupled chemical reaction seemed likely, since reductive S–S bond breaking has several precedents in literature.[3,5,20]

All three previously discussed mechanisms, *viz.* EE, ECE, and EEC, were also feasible for **1** (Scheme S2), and thus in-depth electrochemical studies in combination with DFT computations where carried out to unravel the sequence of events.

The DFT calculated minimum energy structure of **1** (see SI for details) shows a S–S bond length of 2.076 Å and tilting of the two pyridine rings with a C–S–S–C torsion angle φ = 22.3°, which is similar to the experimentally observed values for a S$_2$-bridged benzidine (2.053 Å, φ = 29°),[21] **A** (2.059 Å, φ = 30.4°)[3a] and for **B** (2.056 Å, φ = 32°).[4] The LUMO of **1** has antibonding character with respect to the S–S bond and bonding character with respect to the C–C bond linking the pyridine rings (Fig. 5). Hence single electron reduction of **1** weakens the S–S bond, and relax scan calculations for **1^{red}** reveal a global minimum at a C–S–S–C torsion angle φ = 49.1° with a significantly elongated S–S bond of 2.747 Å; this S–S distance is shorter than the sum of the van der Waals radii (*cf.* r(S) = 1.85 Å)[22] and similar to the distance observed in systems where radical character of a S–S bond has been proposed (*cf.* d(S···S) = 2.777 Å).[23] The SOMO of **1^{red}** exhibits exclusively σ* S–S antibonding character (Fig. 5). While a local energy minimum was also found for a broken S–S bond and *anti* orientation of the pyridine rings (φ = 177.5°), this is much higher in energy (+12.3 kcal/mol) and the barrier for rotation around the central C–C bond is prohibitively high.

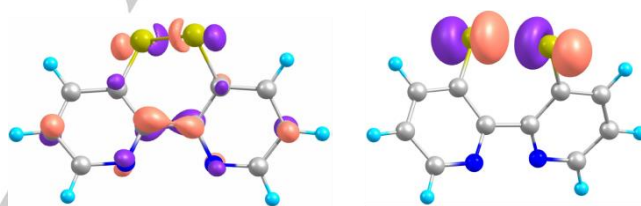**Fig. 5** Left: LUMO of **1** (contour value: 0.08). Right: SOMO of **1^{red}** (contour value: 0.08). See SI for details.
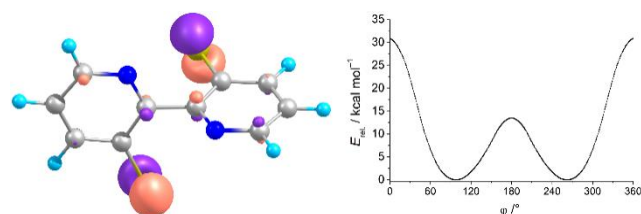

Fig. 6 Left: HOMO of **2**H$_{-2}$ (at global minimum with φ = 94.1°; contour value: 0.08). Right: energy profile for rotation around the central C-C bond of **2**H$_{-2}$. See SI for details.

Further reduction of **1^{red}**, however, results in large geometric changes and S–S bond breaking according to DFT calculations (Fig. 6). The two-electron reduced product of **1**, *viz.* dianionic **2**H$_{-2}$, exhibits a C–S···S–C torsion of φ = 94° and a long S···S separation of 4.398 Å, thus any bonding interactions are no longer present. The close to orthogonal orientation of the pyridine rings in **2**H$_{-2}$ results as a compromise between electrostatic repulsion of the two thiolates and repulsive

interactions between the thiolate and pyridine-N lone pairs. If constrained in close proximity in a *syn* configuration in *N,N'*-chelated metal complexes, one can expect the peripheral thiolates of **2**H$_{-2}$ to be very basic. In summary, the DFT calculation rule out an ECE mechanism for the reduction of **1**, because the first reduction leads to elongation of the S–S bond, but S–S bond breakage occurs only after a second electron is added. Such an EEC mechanism seemed plausible and in line with the proposed reduction sequence of events during reduction of **A**.[3]

Simulation of the CV data was then pursued to experimentally substantiate the proposed EEC mechanism. Simulations were carried out for sweep rates of 0.1 to 10 Vs^{-1}, and the entire curves were simulated. A typical comparison of the experimental and simulated cyclic voltammogram is depicted in Fig. 7, a figure showing the other scan rates can be found in the SI (Fig. S15). Good simulations could be achieved using reasonable values for the various parameters over the entire sweep rate range. The large separation of the reduction and oxidation waves as well as the peak potential shift with increasing scan rates indicates rather slow electron transfer rates, likely due to the significant structural change accompanying the reduction. The initial reduction of **1** to give **1**^{red} exhibits a potential of −1.97 V at an electron transfer rate $k_{s,1}$ of 1×10^{-5} cm/s that is indeed small. The second reduction to give **1**^{red2} occurs at a slightly lower potential of −2.15 V ($k_{s,2}$ = 1×10^{-4} cm/s) and is followed by a fast chemical reaction with a rate constant $k_{c,1}$ ≥ 50 s^{-1} leading to **2**H$_{-2}$ (Scheme 2). The second reduction hence occurs at a more negative potential than the first reduction, in contrast to what has been proposed previously for related dithiins **A** and **B**.[3,5] Fast chemical reaction upon twofold reduction is consistent with S–S bond breaking and twisting of the pyridine units against each other.
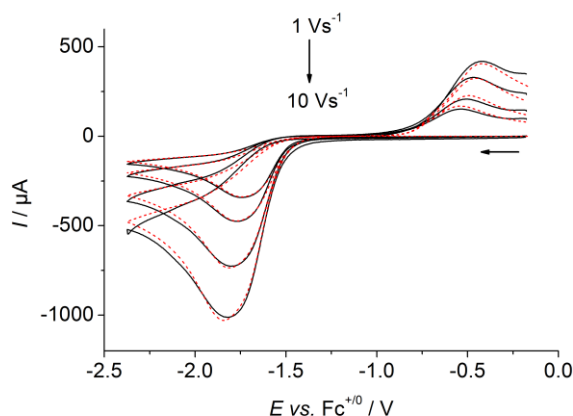
The ratio of the anodic and cathodic peak currents equals 45 %. The anodic feature can be modelled by re-oxidation of **2**H$_{-2}$ at a potential E_3 of −1.92 V ($k_{s,3}$ = 1×10^{-4} cm/s) and subsequent very fast chemical reaction forming **1**^{red} ($k_{c,2}$ ≥ 100 s^{-1}). A further unproductive pseudo first order chemical side reaction has to be considered to successfully model the data ($k_{c,3}$ in Scheme 2), which likely reflects the partial protonation of **2**H$_{-2}$ forming **2**H$_{-1}$ or **2** due to traces of water in the solvent MeCN.[3b] The reverse feature can also be modelled applying an EEC mechanism upon oxidation of **2**H$_{-2}$, that is S–S bond formation occurs not before the second reduction, though, this scenario seems less plausible. A simulation applying an EE mechanism as observed for **B** did not match the CV curves.
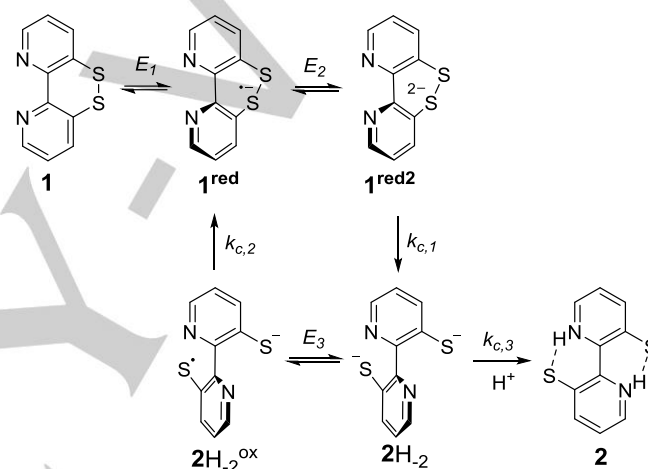
Scheme 2 Proposed mechanism for the reductive S–S bond cleavage reaction of **1** and re-oxidation of **2**H$_{-2}$; E_1 = −1.97 V, E_2 = −2.15 V, E_3 = −1.92 V, $k_{c,1}$ ≥ 50 s^{-1}, $k_{c,2}$ ≥ 100 s^{-1}, $k_{c,3}$ = 0.02 s^{-1}.

Water strongly influences the redox properties of **1** and **2** as revealed by electrochemical measurements conducted in the presence of water. Upon adding 10 eq. of water, the cathodic peak gets much sharper and shifts anodically (Fig. S16). This is even more pronounced in the presence of 100 eq. of water (Fig. S16, S17). The peak current $I_{p,c}$ of the reduction wave increased linearly with the square root of the scan rate (0.1 − 10 Vs^{-1}) indicating a diffusion controlled process (100 eq. water, Fig. S18). The cathodic and anodic waves are largely separated while a linear shift of $E_{p,c}$ with log(v) is still observed, which points to a fast chemical reaction following the reduction (100 eq. water, Fig. S19). Initial inspection of the CV data in the presence of 10 and 100 eq. of water suggested an ECE mechanism, the chemical reaction being first order with regard to water. The steep slope of the reduction wave indicates potential inversion of the first and second reduction process.[5,24] Protonation and bond breaking following the initial reduction as previously suggested for **A**[3b] seemed also reasonable for **1** and therefore we had a closer look on the protonated radical

Fig. 7 Cyclic voltammograms of 3.1 mM **1** in dry MeCN at rt (0.1 M Bu$_4$NPF$_6$); v = 1−10 V/s. black lines: experimental data; red dotted lines: simulation according to Scheme 2 with the parameter values E_1 = −1.97 V, α_1 = 0.4, $k_{s,1}$ = 1×10^{-5} cm/s, E_2 = −2.15 V, α_2 = 0.3, $k_{s,2}$ = 1×10^{-4} cm/s, E_3 = −1.92 V, α_3 = 0.7, $k_{s,3}$ = 1×10^{-4} cm/s, $k_{c,1}$ ≥ 50 s^{-1}, $k_{c,2}$ ≥ 100 s^{-1}, $k_{c,3}$ = 0.02 s^{-1}.

1^{red}H. However, DFT studies of **1^{red}H** revealed a global minimum energy structure in the closed form, because **1^{red}** exhibits a basic N atom of the pyridine unit in contrast to **A**. A local energy minimum was also found for a rotamer with broken S−S bond and *anti* orientation of the pyridine rings (φ = 180°), but this is 6.4 kcal/mol higher in energy (Fig. S43). The S−S distance of ground state **1^{red}H** is much shorter than in **1^{red}** (d(S−S) = 2.11 vs. 2.75 Å) and similar to the S−S bond length in **1**, and the tilting of the two pyridine rings is less pronounced (C−S−S−C torsion angle φ = 27.0°). In fact, the SOMO of **1^{red}H** has no σ* S−S antibonding character as in **1^{red}**, but is of π* orbital type and is localized at the bipyridine unit (Fig. 8). Protonation hence changes drastically the electronic structure of the radical **1^{red}**, but does not induce S−S bond rupture.
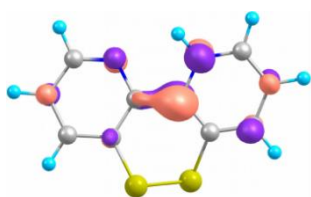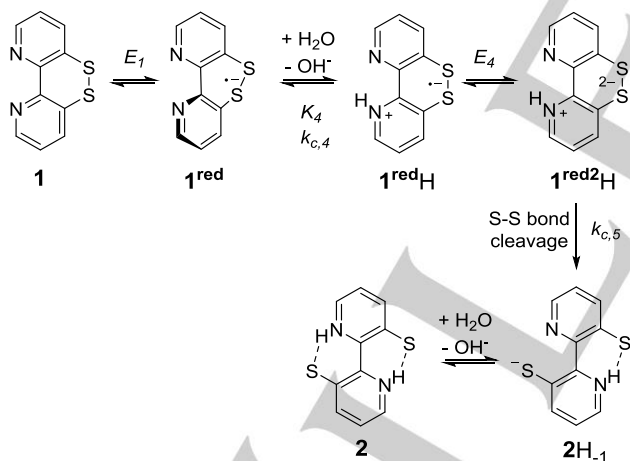

Fig. 8 SOMO of protonated **1^{red}H** (contour value: 0.08). See SI for details.

Since protonation of **1^{red}** does not result in any bond cleavage, we simulated the CV data of **1** in the presence of water by adding to the original model an equilibrium reaction involving **1^{red}** and water, as depicted in Scheme 3.

Scheme 3 Proposed mechanism for the reductive S−S bond cleavage reaction of **1** in the presence of water; E_1 = −1.97 V, α_1 = 0.4, $k_{s,1}$ = 1×10^{-5} cm/s, $E_4 \geq$ −1.9 V, K_4 = 0.001− infinite, $k_{c,4}$ = 3×10^3–3×10^4 M^{-1}s^{-1}, $k_{c,5}$ > 50 s^{-1}. The second protonation equilibrium cannot be simulated as it occurs after the irreversible bond cleavage.

The CV is moderately sensitive to reaction rate $k_{c,4}$ and rather insensitive to the equilibrium constant K_4 of the chemical reaction, because these parameters are interdependent. The fast reaction rate $k_{c,4}$ compensates large changes in the equilibrium constant K_4; therefore only ranges of the two values are given. Reasonable fits could be obtained by using

large second order reaction rate constants ($k_{c,4}$ = 3 × 10^3 − 3 × 10^4 M^{-1}s^{-1}) and equilibrium constants between 0.001 and infinite, the latter describing an irreversible reaction. The generated **1^{red}H** species exhibits a further reduction at a potential of ≥ −1.9 V, hence it is easier to reduce than **1** and non-protonated **1^{red}**. The potential of **1^{red}H** is shifted by at least +250 mV with regard to **1^{red}** due to the charge compensation by protonation. Finally, the S−S bond in **1^{red2}H** breaks with a rate constant $k_{c,5} \geq$ 50 s^{-1}. Fig. 9 shows a representative fit, further scan rates are presented in the SI (Fig. S21, S22, and S23).
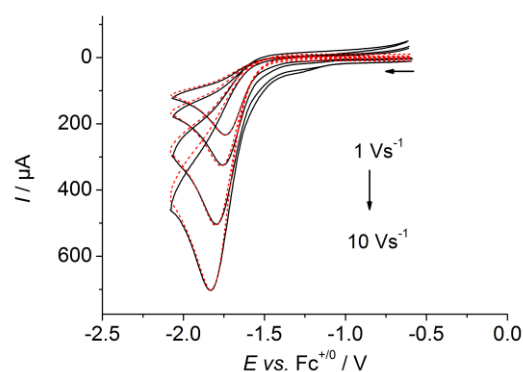

Fig. 9 Cyclic voltammograms of 1.8 mM **1** and 0.21 M water in acetonitrile at rt (0.1 M Bu$_4$NPF$_6$). Black lines: experimental data; red dashed lines: simulation according to Schemes 2 and 3 with the parameter values E_1 = −1.97 V, α_1 = 0.4, $k_{s,1}$ = 1×10^{-5} cm/s, E_2 = −2.15 V, α_2 = 0.3, $k_{s,2}$ = 1×10^{-4} cm/s, $E_4 \geq$ −1.9 V, α_4 = 0.5, $k_{s,4}$ = 1×10^{-4} cm/s, $k_{c,1} \geq$ 50 s^{-1}, $k_{c,2} \geq$ 100 s^{-1}, $k_{c,4}$ = 3.000–30.000 s^{-1}M^{-1}, K_4 = 0.001–infinite, $k_{c,5}$ = 50 s^{-1}M^{-1}.

Conclusions

It has been successfully demonstrated that the new dithiine **1** exhibits two chemically reversible reduction processes and that the potential of the second reduction event can be tuned by protonation. Specifically, thorough electrochemical characterisation of **1** revealed that protonation by a weak acid such as water facilitates the second reduction which then occurs at slightly lower potential than the first one; hence protonation triggers potential inversion. DFT computations indicated that the SOMO of the singly reduced species has dominant S−S antibonding character in the non-protonated form **1^{red}**, but is of π* bipyridinium type in protonated **1^{red}H**. In any case, the S−S bond is still intact in the radical species, while S−S bond breaking occurs only after the second reduction. Indeed, CV data for **1** were simulated successfully by applying an EEC mechanism, or an ECEC mechanism in the presence of water, showing that injection of the second electron provides the driving force for S−S bond rupture. These findings offer interesting prospects for metal complexes of **1** in which the 2,2' bipyridine unit serves as a common N,N' chelate ligand. Such systems may potentially mediate two-electron two-proton conversions via reversible making and breaking of the peripheral S−S bond, electronically coupled to, or triggered by, redox or

photochemical processes involving the metal ion. Because any significant rotation about the central C-C bond will be prevented in complexes of the N,N'-chelating 2,2'-bipyridine derivatives, we expect the two closely spaced thiolates generated upon reduction of metal-bound **1** to readily undergo S-protonation, similar to complexes of 3,3'-dihydroxy-2,2'-bipyridine which forms a stable intramolecular O-H···O hydrogen bond over a wide pH range.[25] Work in that direction is in progress in our laboratories.

Experimental Section

Materials. All used chemicals were reagent grade. 2-bromo-3-hydroxy-pyridine was purchased from Aldrich, and 3,3'-dihydroxy-2,2'-bipyridine was synthetized according to a literature procedure.[26] CH_3CN was freshly distilled for electrochemical measurements. Tetrakis(n-butyl)ammonium hexafluorophosphate was heated at 80 °C under vacuum for 2 days prior to use and stored in the glovebox.

Characterization methods. IR spectra were recorded as KBr pellets on a FTIR Digilab Excalibur Series FTS 3000. UV-vis spectra were recorded with Varian Cary 50 and 5000 spectrophotometers. Steady-state luminescence was measured on a Fluorolog322 instrument from Horiba Jobin–Yvon. NMR Spectra were recorded on Avance DRX 500 (Bruker), Avance 500 Ultrashield (Bruker), Avance 300 (Bruker) and Avance III 300 (Bruker) instruments in D_2O and $CDCl_3$ with residual protons as internal references. Mass spectrometry was performed with a Finnigan MAT 8200 (EI-MS) or a Bruker HTC Ultra (ESI-MS). Elemental analyses were measured by the Analytic Service of the Georg-August-University in Göttingen.

Electrochemistry. Cyclic voltammetry experiments were carried out in CH_3CN with a *Gamry* Reference 600. A silver wire as (pseudo)reference electrode was used with ferrocene as internal standard, a glassy carbon disk electrode as working electrode (*IJ Cambria*, $A = 0.707$ cm²), a Pt wire as auxiliary electrode, and 0.1 m [$^nBu_4N$]PF_6 as supporting electrolyte. All electrochemical measurements were conducted in the glove box under dry dinitrogen, those in the presence of water in a home-made tight CV cell. iR compensation was applied by the positive feedback method, which is implemented in the PHE200 software of *Gamry*. The CV data were simulated with DigiElch 8 FD purchased from *Gamry*.

3,3'-dihydroxy-dimethylthiocarbamoyl-2,2'-bipyridine (I). Compound **I** was synthesized from the commercially available starting material 3,3'-dihydroxy-2,2'-bipyridine in close analogy to protocols developed for other precursors for Newman-Kwart rearrangements.[27] Dry N_2 was bubbled into a solution of 3,3'-dihydroxy-2,2'-bipyridine (660 mg, 3.51 mmol, 1 eq.) in DMF (50 ml) for 30 min. NaH (337 mg, 14.04 mmol, 4 eq.) was the added and the reaction mixture stirred for 1 hour under inert conditions. The intense green fluorescence of 3,3'-dihydroxy-2,2'-bipyridine gradually changes to blue indicative of formation of the deprotonated species. Then dimethylthiocarbamoyl chloride (2.169 g, 17.55 mmol, 5 eq.) was added and the solution heated to 85°C and stirred overnight under N_2 atmosphere. The yellow solution turned to dark brown and fluorescence vanished. The solution was then allowed to cool to rt and quenched with 1% aqueous KOH (300) and extracted with DCM (4x100 ml). The combined organic phases were evaporated to dryness under reduced pressure. The resulting brown oil was purified by column chromatography (silica gel) and the product eluted with hexanes/ethyl acetate 1:1 (R_f with ethyl acetate 0.22). The product **I** was finally recrystallized from DCM/hexanes to yield a white solid (yield 52%). Anal. Calc. for $C_{16}H_{18}N_4O_2S_2$ (%): C 53.02, H 5.00, N 15.46, S 17.69. Found: C 53.05, H 4.93, N 15.65, S 17.85. IR (KBr pellets): 3065 (w), 2940 (w), 2880 (w), 1627 (w), 1537 (s), 1454 (w), 1441 (w), 1419 (s), 1394 (s),

1289 (s), 1240 (s), 1202 (s), 1178 (m), 1126 (s), 1106 (m), 1060 (w), 1039 (m), 819 (w), 791 (w), 756 (w), 687 (w), 619 (w) cm^{-1}. ^{1}H-NMR (300 MHz, $CDCl_3$): $\delta = 8.52$ (2, dd, 2H, $J_{2-3} = 4.6$ Hz, $J_{2-4} = 1.4$ Hz), 7.76 (4, dd, 2H, $J_{4-3} = 8.2$ Hz, $J_{4-2} = 1.4$ Hz), 7.38 (3, dd, 2H, $J_{3-4} = 8.3$ Hz, $J_{3-2} = 4.7$ Hz), 3.29 (11, s, 6H), 3.03 (12, s, 6H). ^{13}C-NMR (75 MHz, $CDCl_3$) δ 185.99 (8), 148.74 (5), 148.63 (6), 146.09 (2), 133.03 (4), 123.47 (3), 43.35 (11), 38.97 (12). ^{15}N-NMR (30 MHz, $CDCl_3$): $\delta = -62.8$ (1), -262.2 (14). ESI-MS (MeCN) m/z (%): [M+H]$^+$ 363.1 (100). UV-vis (CH_3CN): λ_{max} [nm] (ε_{rel} [L mol^{-1}cm^{-1}]) = 251 (34600).

Compounds II, III and IV. These were synthesized following the general procedure for Newman-Kwart rearrangements.[26] After extensive optimization of the reaction conditions, best results were obtained by heating neat **I** (100 mg) to 280°C under N_2 atmosphere for 7 min. ^{1}H NMR spectroscopy suggested the black product mixture to contain **III** (~36%), **IV** (~26%) and **II** (~16%) besides some remaining **I** and other unidentified side products. The compounds were separated by column chromatography (silica gel, hexanes/diethyl acetate 1:1). The first fraction is **III** (R_f in ethyl acetate ~0.71). Anal. Calc. for $C_{10}H_6N_2S$ (%): C 64.29, H 3.60, N 14.37, S 16.40. Found: C 64.12, H 3.82, N 14.07, S 16.18. IR (KBr pellets): 3046 (w), 2925 (w), 2956 (w), 1541 (s), 1462 (w), 1395 (s), 1335 (w), 1288 (m), 1225 (w), 1196 (m), 1146 (m), 1067 (s), 1040 (w), 1031 (w), 986 (w), 967 (w), 814 (w), 801 (m), 789 (s), 733 (s), 696 (m), 621 (m) cm^{-1}. ^{1}H-NMR (300 MHz, $CDCl_3$): $\delta = 8.91$ (2, dd, 2H, $J_{2-3} = 4.6$ Hz, $J_{2-4} = 1.4$ Hz), 8.23 (4, dd, 2H, $J_{4-3} = 8.2$ Hz, $J_{4-2} = 1.4$ Hz), 7.48 (3, dd, 2H, $J_{3-4} = 8.2$ Hz, $J_{3-2} = 4.5$ Hz). ^{13}C-NMR (75 MHz, $CDCl_3$): $\delta = 150.54$ (6), 148.08 (2), 134.63 (5), 131.09 (4), 120.40 (3). ^{15}N-NMR (30 MHz, $CDCl_3$): $\delta = -78$ (1). ESI-MS (MeCN) m/z (%): [M+H]$^+$ 187.03 (100). UV-vis (CH_3CN): λ_{max} [nm] (ε_{rel} [L mol^{-1}cm^{-1}]) = 298 (14300), 290 (sh), 257 (10700), 228 (38200), 210 (15800). The second fraction is the starting material **I** (R_f in ethyl acetate ~0.58). The third fraction is the singly rearranged product **IV** (R_f in ethyl acetate ~0.26). Anal. Calc. for $C_{16}H_{18}N_4O_2S_2$ (%): C 53.02, H 5.00, N 15.46. Found: C 53.25, H 5.10, N 15.17. IR (KBr pellets): 3055 (w), 3014 (w), 2956 (w), 2918 (w), 2856 (w), 1635 (m), 1594 (s), 1552 (s), 1458 (m), 1432 (m), 1371 (s), 1327 (m), 1277 (w), 1218 (w), 1156 (w), 1106 (w), 1066 (w), 988 (w), 970 (w), 903 (w), 826 (s), 748 (w), 684 (m), 669 (w), 530 (m), 414 (w) cm^{-1}. ^{1}H-NMR spectrum (300 MHz, $CDCl_3$): $\delta = 8.61$ (2, dd, 1H, $J_{2-3} = 4.6$ Hz, $J_{2-4} = 1.7$ Hz), 8.52 (2', dd, 1H, $J_{2-3} = 4.7$ Hz, $J_{2-4} = 1.4$ Hz), 7.97 (4, dd, 1H, $J_{3-4} = 8.0$ Hz, $J_{2-4} = 1.7$ Hz), 7.77 (4', dd, 1H, $J_{3-4} = 8.3$ Hz, $J_{2-4} = 1.4$ Hz), 7.37 (3', dd, 1H, $J_{3-2} = 4.7$ Hz, $J_{3-4} = 8.3$ Hz), 7.35 (3, dd, 1H, $J_{3-2} = 4.7$ Hz, $J_{3-4} = 8.0$ Hz), 3.21 (11', s, 3H), 2.89 (11-12, s, 6H), 2.86 (12', s, 3H). ^{13}C-NMR (200 MHz, $CDCl_3$): $\delta = 185.12$ (8'), 164.88 (8), 157.52 (6), 150.44 (6'), 148.55 (2), 147.78 (5'), 145.77 (2'), 145.69 (4), 132.69 (4'), 127.01 (5), 123.27 (3), 123.23 (3'), 42.93 (11'), 38.37 (12'), 36.88 (11-12). ^{15}N-NMR (30 MHz, $CDCl_3$): $\delta = -63.2$ (1), -65.7 (12), -262.5 (14). ESI-MS (MeCN) m/z (%): [M+H]$^+$ 363.09 (100). The last fraction is **II** (R_f in ethyl acetate ~0.17). Anal. Calc. for $C_{16}H_{18}N_4O_2S_2$ (%): C 53.02, H 5.00, N 15.46, S 17.69. Found: C 53.67, H 4.97, N 15.34, S 17.60. IR (KBr pellets): 3056 (w), 3017 (w), 2916 (w), 1626 (s), 1553 (m), 1477 (w), 1459 (w), 1434 (w), 1400 (s), 1369 (s), 1257 (m), 1099 (m), 1072 (w), 1043 (m), 1037 (w), 906 (w), 813 (w), 801 (m), 786 (w), 774 (w), 685 (s), 648 (w), 623 (w), 525 (w) cm^{-1}. ^{1}H-NMR (300 MHz, $CDCl_3$): $\delta = 8.65$ (2, dd, 2H, $J_{2-3} = 4.8$ Hz, $J_{2-4} = 1.6$ Hz), 8.01 (4, dd, 2H, $J_{4-3} = 8.0$ Hz, $J_{4-2} = 1.6$ Hz), 7.39 (3, dd, 2H, $J_{3-4} = 8.0$ Hz, $J_{3-2} = 4.8$ Hz), 2.91 (11, s, 12H). ^{13}C-NMR (75 MHz, $CDCl_3$): $\delta = 165.15$ (8), 159.80 (6), 148.88 (2), 145.33 (4), 126.52 (5), 123.42 (3), 37.04 (11). ^{15}N-NMR (30 MHz, $CDCl_3$): $\delta = -66.0$ (12), -285.5 (18). ESI-MS (MeCN) m/z (%): [M+H]$^+$ 368.09 (100).

[1,2]dithiino[4,3-b:5,6-b']dipyridine (1). Removal of the thiocarbamoyl groups from **II** was performed according to common procedures, using LiAlH$_4$.[26] To a solution of LiAlH$_4$ (190 mg, 5 mmol) in dry THF under N_2 atmosphere was added **II** (234 mg, 0.645 mmol) dissolved in dry THF (15 ml). The reaction mixture was stirred under N_2 atmosphere for 30 min and then heated to 50°C for 3 h. After cooling down to 0°C, 0.1 M aqueous HCl (10 ml) was added slowly until the solution turned to intense red. The dithiol **2** was extracted with DCM (4 x 50 ml) and the

combined organic phases were exposed to air, causing the colour of the solution to turn yellow. The solution was concentrated in *vacuo* and the yellow oil was chromatographed on silica gel with ethyl acetate. **1** was isolated as a yellow oil (R_f in ethyl acetate ~0.1). ^{1}H-NMR (300 MHz, CDCl$_3$): δ = 8.68 (2, dd, 2H, $J_{2\text{-}3}$ = 4.6 Hz, $J_{2\text{-}4}$ = 1.6 Hz), 7.72 (4, dd, 2H, $J_{4\text{-}3}$ = 7.9 Hz, $J_{4\text{-}2}$ = 1.6 Hz), 7.22 (3, dd, 2H, $J_{3\text{-}4}$ = 7.9 Hz, $J_{3\text{-}2}$ = 4.7 Hz). ^{13}C-NMR (75 MHz, CDCl$_3$): δ = 153.08 (6), 149.44 (2), 136.01 (4), 133.94 (5), 123.67 (3). ^{15}N-NMR (30 MHz, CDCl$_3$): δ -70.6 (1). ESI-MS (MeCN) *m/z* (%): [M+H]$^+$ 219.00 (100%), [M+Na]$^+$ 240.99 (30%). UV-vis (CH$_3$CN): λ_{max} [nm] (ε_{rel} [L mol^{-1}cm^{-1}]) = 360 (360), 302 (5900), 265 (9400).

3,3'-dithiol-2,2'-bipyridine (2). The dithiol was synthesized following the procedure for **1**, but the reaction mixture was kept under inert conditions throughout. LiAlH$_4$ (200 µL of a 1.0 M solution in THF, 200 µmol) was added to **II** (8 mg, 22 µmol) under an atmosphere of dry Ar and the reaction mixture stirred for 5 min, then heated to 50°C for 3 h. After cooling to 0°C, 0.1 M aqueous HCl (3 ml) were added slowly. The aqueous phase was further diluted with 0.1 M aqueous HCl (50 ml) and the solution turned intense red. **2** was extracted with DCM (6 x 5 ml) under Ar atmosphere. The solvent was then removed under reduced pressure and the remaining red solid was recrystallized from a DCM/toluene mixture. ^{1}H-NMR (300 MHz, CDCl$_3$): δ = 8.39 (2, dd, 2H, $J_{2\text{-}3}$ = 8.3 Hz, $J_{2\text{-}4}$ = 1.6 Hz), 8.01 (4, dd, 2H, $J_{4\text{-}3}$ = 5.1 Hz, $J_{4\text{-}2}$ = 1.6 Hz), 7.31 (3, dd, 2H, $J_{3\text{-}4}$ = 5.1 Hz, $J_{3\text{-}2}$ = 8.3 Hz).

Acknowledgements

[1]   (a) C. S. Sevier and C. A. Kaiser, *Nat. Rev. Mol. Cell Biol.*, **2002**, *3*, 836-847; (b) S. W. Ragsdale, N. Gupta, I. Bagai, A. M. Spencer and E. Carter, in *Handbook of Porphyrin Science*, (Eds. K. M. Kadish, K.M. Smith, R. Guilard), **2014**, *30*, 31-54.

[2]   G. Capozzi and G. Modena, in *The Chemistry of the Thiol Group*, (Ed. S. Patai), John Wiley & Sons, **1974**, *17*, 785-839.

[3]   (a) I. Llarena, A. C. Benniston, G. Izzet, D. B. Rewinska, R. W. Harrington and W. Clegg, *Tetrahedron Lett.*, **2006**, *47*, 9135-9138; (b) A. C. Benniston, B. D. Allen, A. Harriman, I. Llarena, J. P. Rostron and B. Stewart, *New J. Chem.*, **2009**, *33*, 417-427.

[4]   A. C. Benniston, J. Hagon, X. He, S. Yang and R. W. Harrington, *Org. Lett.*, **2012**, *14*, 506-509.

[5]   G. B. Hall, R. Kottani, G. A. N. Felton, T. Yamamoto, D. H. Evans, R. S. Glass and D. L. Lichtenberger, *J. Am. Chem. Soc.*, **2014**, *136*, 4012-4018.

[6]   (a) S. Antonello, K. Daasbjerg, H. Jensen, F. Taddei and F. Maran, *J. Am. Chem. Soc.*, **2003**, *125*, 14905–14916; (b) F. Maran, D. D. M. Wayner and M. S. Workentin, *Adv. Phys. Org. Chem.*, **2001**, *36*, 85.

[7]   2,2'-bipyridine-3,3'-dithiol has so far only been mentioned in a few patents, without any details: (a) Y. Lu,

[8]   U.S. Pat. Appl. Publ. **2015**, US 20150336884 A1 20151126; (b) J. Y. Baek, S. H. lee, J. U. Lee, D. W. Lee and S. H. Kim, Repub. Korean Kongkae Taeho Kongbo **2014**, KR 2014121991 A 20141017.

[8]   (a) C. Kaes, A. Katz and M. W. Hosseini, *Chem. Rev.* **2000**, *100*, 3553–3590; (b) G. R. Newkome, A. K. Patri, E. Holder and U. S. Schubert, *Eur. J. Org. Chem.*, **2004**, 235-254; (c) A. P. Smith and C. L. Fraser, in: *Comprehensive Coordination Chemistry II*, (Eds. J. A. McLeverty, T. J. Meyer), Elsevier, **2004**, *1*, 1-23.

[9]   (a) V. W. Manner, A. D. Lindsay, E. A. Mader, J. N. Harvey and J. M. Mayer, *Chem. Sci.*, **2012**, *3*, 230-243; (b) E. A. Mader, E. R, Davidson and J. M. Mayer, *J. Am. Chem. Soc.*, **2007**, *129*, 5153-5166; (c) A. Wilting, M. Kügler and I. Siewert, *Inorg. Chem.*, **2016**, *55*, 1061–1068. (d) A. Pannwitz, A. Prescimone and O. S. Wenger, *Eur. J. Inorg. Chem.*, **2017**, 609-615.

[10]   L. Stefaniak, G. A. Webb, C. Brevard, M. Bourdonneau, R. Lejeune, L. Thunus and C. L. Lapiere, *Magn. Res. Chem.*, **1985**, *23*, 790-792.

[11]   (a) G. Ramirez-Galicia, G. Perez-Gallardo and M. Rubio, *J. Mol. Struc. THEOCHEM*, **2001**, *542*, 1-6; (b) A. Guven, *Int. J. Mol. Sci.*, **2005**, *6*, 257-275.

[12]   B. Dakova, P. Carbonnelle, A. Walcarius, L. Lamberts and M. Evers, *Electrochim. Acta*, **1992**, *37*, 725–729.

[13]   A. Y. Zheltov, V. Y. Rodinonov and B. I. Stepanov, *Zhurnal Organicheskoi Khimii*, **1975**, *11*, 1304-1311.

[14]   N. Armaroli, L. De Cola, V. Balzani, J.-P- Sauvage, C. O. Dietrich-Buchecker and J.-M. Kern, *J. Chem. Soc. Faraday Trans.*, **1992**, *88*, 553-556.

[15]   S. Babic, A. J. M. Horvat, D. Mutavdzic Pavlovic and M. Kastelan-Macan, *Trends Anal. Chem.*, **2007**, *26*, 1043-1061.

[16]   D.R. Lide, *CRC Handb. Chem. Physics*, **2005**, 42–51.

[17]   Y. Couturier and C. Petitfaux, *Bull. Soc. Chim. Fr.*, **1974**, 855–862.

[18]   (a) E. Block, M. Birringer, R. DeOrazio, J. Fabian, R. S. Glass, C. Guo, C. He, E. Lorance, Q. Qian, T. B. Schroeder, Z. Shan, M. Thiruvazhi, G. S. Wilson and J. Zhang, *J. Am. Chem. Soc.*, **2000**, *122*, 5052–5064; (b) A. Wakamiya, T. Nishinaga and K. Komatsu, *J. Am. Chem. Soc.*, **2002**, *124*, 15038–15050; (c) H. Hennig, F. Schumer, J. Reinhold, H. Kaden, W. Oelssner, W. Schroth, R. Spitzner and F. Hartl, *J. Phys. Chem. A.*, **2006**, *110*, 2039–2044.

[19]   A. J. Bard and L. R. Faulkner, *Electrochemical Methods: Fundamentals and Applications*, Wiley, New York, **2001**.

[20]   (a) S. Antonello, K. Daasbjerg, H. Jensen, F. Taddei, F. Maran, *J. Am. Chem. Soc.* **2003**, *125*, 14905–14916; (b) F. Maran, D. D. M. Wayner, M. S. Workentin, *Adv. Phys. Org. Chem.* **2001**, *36*, 85.

[21]   Q. Zhu-Ohlbach, R. Gleiter, F. Rominger, H. Schmidt and T. Reda, *Eur. J. Org. Chem.*, **1998**, 2409–2416.

[22]   S. S. Batsanov, *Inorg. Mater.*, **2001**, *37*, 871–885.

[23]   S. Yao, C. Milsmann, E. Bill, K. Wieghardt and M. Driess, *J. Am. Chem. Soc.*, **2008**, *130*, 13536.

[24]   (a) D. H. Evans, K. Hu, *J. Chem. Soc. Faraday Trans.* **1996**, *92*, 3983-3990; (b) Y. C. Chung, Y. J. Tu, S. H. Lu, W. C. Hsu, K. Y. Chiu, Y. O. Su, *Org. Lett.* **2011**, *13*, 2826–2829.

[25]   A. M. W. C. Thompson, J. C. Jeffery, D. J. Liard, M. D. Ward, *J. Chem. Soc., Dalton Trans.* **1996**, 879-884.

[26]   C. Naumann, H. Langhals, H. *Synthesis* **1990**, 279.

[27]   (a) Cossu, S.; De Lucchi, O.; Fabbri, D.; Valle, G.; Painter, G. F.; Smith, R. A. J. *Tetrahedron* **1997**, *53*, 6073. (b) Moseley, J. D.; Sankey, R. F.; Tang, O. N.; Gilday, J. P.

Tetrahedron **2006**, *62*, 4685. (c) Theil, H.; Frohlich, R.; Glaser, T. *Z. Naturforsch*. **2009**, *64b*, 1633.

FULL PAPER

Entry for the Table of Contents

FULL PAPER

Electrochemical investigation of a new dithiine that amalgamates the 2e⁻/2H⁺ disulfide/dithiol couple with the 2,2'-bipyridine scaffold shows that protonation by a weak acid such as water facilitates the second reduction and triggers potential inversion while inducing a switch from an EEC mechanism to an ECEC mechanism.
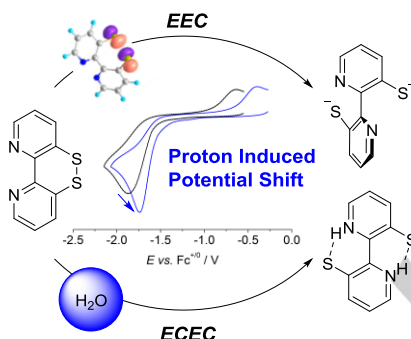
Mauricio Cattaneo[*] Christine E. Schiewer, Anne Schober, Sebastian Dechert, Inke Siewert,[*] Franc Meyer[*]

Page No. – Page No.

2,2'-Bipyridine Equipped with a Disulfide/Dithiol Switch for Coupled Two Electron and Proton Transfer